



A Prognostic Nomogram Combining Immune-Related Gene Signature and Clinical Factors Predicts Survival in Patients With Lung Adenocarcinoma

Congkuan Song^{1,2}, Zixin Guo^{1,2}, Donghu Yu^{1,3}, Yujin Wang^{1,2}, Qingwen Wang^{1,2}, Zhe Dong^{1*} and Weidong Hu^{1,2*}

¹ Department of Thoracic Surgery, Zhongnan Hospital of Wuhan University, Wuhan, China, ² Hubei Key Laboratory of Tumor Biological Behaviors & Hubei Cancer Clinical Study Center, Wuhan, China, ³ Department of Biological Repositories, Zhongnan Hospital of Wuhan University, Wuhan, China

OPEN ACCESS

Edited by:

Qing Zhou,

Guangdong Provincial People's Hospital Lung Cancer Institute, China

Reviewed by:

Jai Narendra Patel,

Levine Cancer Institute, United States

Juan Hui Wang,

Affiliated Cancer Hospital of Zhengzhou University, China

*Correspondence:

Zhe Dong

136617338@qq.com

Weidong Hu

huwd@whu.edu.cn

Specialty section:

This article was submitted to

Thoracic Oncology,

a section of the journal

Frontiers in Oncology

Received: 21 April 2020

Accepted: 23 June 2020

Published: 06 August 2020

Citation:

Song C, Guo Z, Yu D, Wang Y, Wang Q, Dong Z and Hu W (2020) A Prognostic Nomogram Combining Immune-Related Gene Signature and Clinical Factors Predicts Survival in Patients With Lung Adenocarcinoma. *Front. Oncol.* 10:1300. doi: 10.3389/fonc.2020.01300

The existence of tumor heterogeneity and complex carcinogenic mechanisms in lung adenocarcinoma (LUAD) make the most commonly used TNM staging system unable to well-interpret the prognosis of patients. Using transcriptome profiling and clinical data from The Cancer Genome Atlas (TCGA) database, we constructed an immune signature based on a multivariate Cox analysis (stepwise model). We estimated the half-maximal inhibitory concentration (IC50) of chemotherapeutic drugs in patients according to the pRRophetic algorithm. Gene-set variation analysis (GSVA) was used to reveal pathway enrichment between groups. Moreover, immune microenvironment landscape was described by single-sample gene-set enrichment analysis (ssGSEA) and CIBERSORT and systematically correlated with genomic of these patients. A prognostic nomogram combining the immune signature and TNM stage to predict the prognosis was developed by multivariate Cox regression. The novel signature with four immune-related genes (MAL, MS4A1, OAS1, and WFDC2) had good robustness, which can accurately distinguish between high- and low-risk patients. Compared with low-risk patients, high-risk patients with a worse prognosis (5-year OS: 46.5 vs. 59.4%, $p = 0.002$) could benefit more from immunotherapy and the application of common chemotherapeutic agents such as cisplatin and paclitaxel (Wilcoxon test, all $p < 0.05$). There were significant differences in tumor immune microenvironment and metabolic pathways between the two groups. Additionally, the constructed nomogram had reliable predictive performance with the C-index of 0.725 (95% CI = 0.668–0.781) in the development set ($n = 500$), 0.793 (95% CI = 0.728–0.858) in the internal validation set ($n = 250$) and 0.679 (95% CI = 0.644–0.714) in the external validation set ($n = 442$). The corresponding calibration curves also showed good consistency. To sum up, we developed an immune-related gene signature and comprehensively evaluated LUAD immune landscape and metabolic pathways. Effective differentiation of high- and low-risk patients and accurate construction of nomogram would be helpful to the development of individualized treatment strategies.

Keywords: lung adenocarcinoma, immune related gene, prognosis, signature, nomogram

INTRODUCTION

Lung cancer is the most common malignancy, with morbidity and mortality ranking first in the world, according to global data released by the International Center for Cancer Research in 2020 (1). Lung cancer is divided into non-small cell lung cancer (NSCLC) and small cell lung cancer (SCLC). As the most common subtype of NSCLC (2), lung adenocarcinoma (LUAD) has complex carcinogenic mechanisms and obvious tumor heterogeneity. Due to the continuous improvement in the diagnosis and treatment of LUAD in recent years, especially the rise of immunotherapy, the prognosis of patients has improved significantly. However, the search for new models of diagnosis and treatment to benefit cancer patients has been the focus of oncologists. It is still necessary to further understand the occurrence and progression of LUAD and to identify strong prognostic biomarkers for LUAD.

Immune-related genes have great significance in the immune mechanism and immune function of the body. As we know, cancer is an extremely complex disease involving interactions between tumor and immune system (3). Immunotargeted therapy has played greatly important roles in improving the prognosis of patients with malignant tumors (4, 5). Nevertheless, the treatment can only be applied to some patients, and there are obvious individual differences in the therapeutic effect of this method (6, 7), which further illustrates the existence of tumor heterogeneity and the complexity of carcinogenic mechanisms. The expression of immune-related genes and the density and type of tumor immune infiltrating cells have been widely studied as prognostic biomarkers of lung cancer (8–10). However, the roles of immune-related genes involved in tumor immune microenvironment are still not fully recognized. In this study, a novel immune signature was constructed. We further revealed the differences in the immune microenvironment between high- and low-risk patients and well-predicted the efficacy of chemotherapy and immunotherapy in both groups. In addition, gene-set variation analysis (GSVA) was also used to explore the molecular mechanisms leading to significantly differential prognosis in high- and low-risk patients. Moreover, we developed a nomogram that can accurately predict the prognosis of patients to improve the efficacy of individualized prediction, which may provide a reference for clinicians to formulate more rational treatment strategies.

MATERIALS AND METHODS

Data Source and Preprocessing

The transcriptome profiling data for 535 cases of lung tumor tissue and 59 cases of lung normal tissue were downloaded

Abbreviations: LUAD, Lung adenocarcinoma; OS, Overall survival; TCGA, The Cancer Genome Atlas; GEO, Gene Expression Omnibus; CI, Confidence interval; HR, Hazard ratio; ROC, Receiver operating characteristic; AUC, Area under the curve; C-index, Concordance index; CTLA-4, Cytotoxic T-lymphocyte associated 4; PD-1, Programmed cell death 1; PD-L1, Programmed cell death-ligand 1; TMB, Tumor mutational burden; GSVA, Gene-set variation analysis; GSEA, Gene-set enrichment analysis.

directly from the Cancer Genome Atlas (TCGA) Genomic Data Commons Data Portal (<https://portal.gdc.cancer.gov/>, updated until March 05, 2020). The same method was also used to extract the corresponding clinical data (including age, sex, T stage, N stage, TNM stage, survival time, and status). Additionally, RNA expression profiles and clinical information of 443 LUAD patients in the GSE68465 dataset (11) were downloaded from the Gene Expression Omnibus (GEO) database (<https://www.ncbi.nlm.nih.gov/geo/>).

Acquisition of Immune-Related Genes

The immune-related gene sets (IMMUNE_RESPONSE and IMMUNE_SYSTEM_PROCESS) were extracted from the Molecular Signatures Database (MSigDB) (<https://www.gsea-msigdb.org/gsea/msigdb/index.jsp>). There were 332 immune-related genes in these two genomes. To increase the available genes, we also downloaded a total of 2,498 immune-related genes in the Gene List from ImmPort (<http://www.immport.org/>). After deleting duplicate genes, 1,986 genes were finally used for the next analysis. We obtained immune-related genes and their expression profiles in combination with mRNA gene sets extracted from the TCGA database.

Differentially Expressed mRNAs (DEMs) in Lung Normal and Tumor Tissues

DEMs between lung normal and tumor tissues were identified by differential expression analysis using the “limma” package in R (12). $|\log_2 \text{FC (fold-change)}| > 1$ and $P < 0.05$ were set as the thresholds for screening DEMs. The common DEMs of the two databases (TCGA and GEO) were used for further analysis.

GO and KEGG Enrichment Analyses of the Common DEMs

To explore in depth the possible biological processes (BP), cellular components (CC), molecular functions (MF), and pathways of the common DEMs, we carried out GO and KEGG enrichment analysis utilizing the “clusterProfiler” package in R (13) with a statistical threshold of $p < 0.05$.

Screening of Immune-Related Genes Affecting Prognosis

In order to identify prognosis-related genes, the patients without accurate survival data (e.g., survival time = 0 day and unknown) were removed from this study. Finally, 500 patients with detailed survival information were included in the study. Using univariate Cox analysis, we evaluated the association of the common DEMs with OS of LUAD patients. Only these genes with $p < 0.05$ in both two databases (TCGA and GEO) were considered as candidate immune-related genes affecting prognosis.

Construction and Evaluation of Immune-Related Gene Signature

Through a multivariate Cox analysis (stepwise model), we filtered these candidate immune-related genes affecting prognosis. Akaike information criterion (AIC) was used to avoid overfitting. We selected the genes with the highest likelihood ratio and lowest AIC values and estimated the β regression coefficients. Based on

the β regression coefficients and expression values of the filtered genes, we calculated the risk score of each sample according to the following formula (14):

$$\text{riskScore} = \sum_{i=1}^n \text{Coef}_i * \text{Expression}_i,$$

where Coef_i was the β regression coefficients obtained from multivariate Cox analysis and Expression_i was the expression of the immune-related genes in the signature. With the median risk score as the cutoff point, patients were divided into high- and low-risk groups. The Kaplan–Meier method was performed to assess the survival differences between the two groups. To further assess the specificity and sensitivity of the immune-related gene-based signature, the ROC curves were drawn and the corresponding AUC values were also calculated. Additionally, we also used the same method to verify the prognostic performance in the internal and external validation datasets. A specific process for constructing this signature is shown in **Figure 1**.

Evaluation of the Sensitivity of Chemotherapeutic Agents

To predict the half-maximal inhibitory concentration (IC50) of chemotherapy drugs in the high- and low-risk groups of LUAD patients and to infer the sensitivity of the different patients, we used the “pRRophetic” package in R. By constructing the ridge regression model based on Genomics of Drug Sensitivity in Cancer (GDSC) (www.cancerrxgene.org/) cell line expression spectrum and TCGA gene expression profiles, the package could apply pRRophetic algorithm to predict drug IC50 (15).

Prediction of Immunotherapy Efficacy

To explore the relationship between the immune signature and immunotherapeutic efficacy, we adopted two computational methods to infer the immunotherapeutic response of LUAD patients at low and high risk. First, we downloaded the mutation data of LUAD from the TCGA database and calculated the tumor mutational burden (TMB) of each sample. The mutation data was divided into two groups by high- and low-risk samples. Second, an online tool named Tumor Immune Dysfunction and Exclusion (TIDE) (<http://tide.dfci.harvard.edu>) was applied to

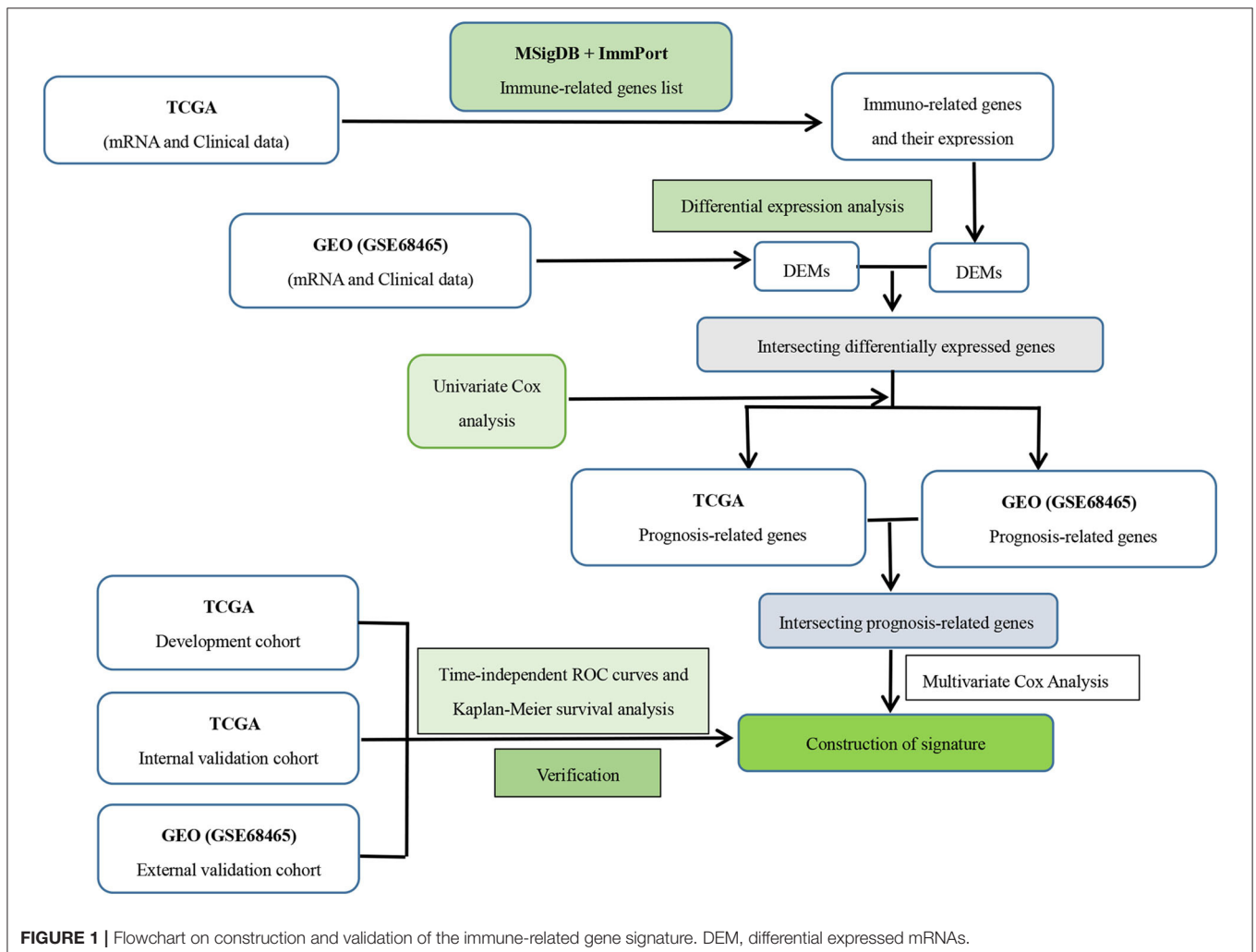


FIGURE 1 | Flowchart on construction and validation of the immune-related gene signature. DEM, differentially expressed mRNAs.

infer the anti-PD1 and anti-CTLA4 immunotherapeutic response of each sample based on the transcriptome profiles of the TCGA-LUAD cohort (16).

Exploration of Tumor Immune Landscape

We obtained a set of marker genes related to immune cell types, including different immune cells, immune-related pathways, and functions from Bindea et al. ssGSEA is a feasibility approach, which can apply the characteristics of immune cell population expression to individual cancer samples and can calculate the rank value of each gene according to the expression profile for subsequent statistical analysis (17, 18). In this study, the “GSVA” package in R (19) was utilized with the ssGSEA method. Moreover, the “estimate” package in R was applied to evaluate the immune score, stromal score, and tumor purity of each sample in the high- and low-risk groups.

Moreover, as a wildly proposed computational algorithm, “Cell type Identification By Estimating Relative Subsets Of RNA Transcripts (CIBERSORT)” (20) (<https://cibersort.stanford.edu>) was also used to predict immune-infiltrating cells of each LUAD sample in our study. The proportion of 22 immune-infiltrating cells in each sample can be obtained by inputting the expression data of the samples. Then, the samples with $p < 0.05$ were selected for further analysis. Human leukocyte antigen (HLA) was also applied to validate the differences between the two groups. In addition, Spearman correlation analysis was used to explore the relationship between four immune-related genes and risk score and immune infiltration.

Gene-Set Variation Analysis

Using the “GSEABase” package in R, we applied gene-set variation analysis (GSVA) that was predominantly performed on the 50 hallmark pathways described in the MSigDB, where each pathway-related gene set was trimmed to contain only unique genes to reduce pathway overlap and pathway redundancy and most genomes retained 70% of the genes involved (21). MSigDB is a collection of annotated gene sets for use with GSEA software. The MSigDB gene sets are divided into 8 major collections (H, C1–C7). We downloaded “c5.all.v7.0.symbols” (GO gene sets that contain genes annotated by the same GO term). The C5 collection was divided into three subcollections based on GO ontologies: biological process (BP), cellular component (CC), and molecular function (MF). To reveal pathway enrichment between low- and high-risk patients, we used the “GSVA” package in R (19) to evaluate t score and assign pathway activity conditions. Moreover, “limma” package in R was also applied to display distinctions in pathway activation between low- and high-risk groups.

The Relationship Between Immune-Related Genes and Transcription Factors

We acquired a transcription factor (TF) list from a web application named Cistrome (<http://cistrome.org/>) and then integrated with the mRNA expression matrix from the TCGA database to derive these TFs’ expression level. We examined the correlation between the expression level of the immune-related

genes in the signature and each TF using two-sided Pearson correlation coefficients and the Z-test. The TFs positively or negatively correlated with the four immune-related genes were considered as immune-related gene-associated TFs ($|\text{Pearson correlation coefficients}| > 0.3$ and $P < 0.001$).

Clinical Correlation and Independent Prognostic Analysis

To better understand the impact of the signature and clinical features on patient outcomes, the univariate and multivariate Cox analyses were performed, which may reveal independent prognostic factors in LUAD patients. In addition, the correlation between the immune-related genes in the signature and clinical features was further explored.

Construction and Verification of a Prognostic Nomogram

Based on the multivariate Cox analysis, we developed a nomogram for predicting LUAD prognosis in the TCGA database. This nomogram incorporated two predictors, namely, risk score and TNM stage. To further verify the predictive power of this nomogram, we used the 50% LUAD samples randomly selected from the entire TCGA database as internal validation dataset ($n = 250$) and the GSE68465 dataset from the GEO database as external validation dataset ($n = 442$). The C-index and calibration plots were used to assess the performance of the established nomogram.

Statistical Analysis

All statistical analysis was conducted in R software 3.6.0. All categorical variables were expressed as number (percentage). The Wilcoxon rank-sum test was performed to compare the differences between groups of continuous data. The relationships between immune-related genes and risk score and immune infiltration were determined by the Spearman’s correlation analysis. The Kaplan–Meier method was used to survival analysis, where the log-rank test was applied to compare the survival distribution. The Cox proportional hazard model was performed to estimate the β regression coefficient, hazard ratios, p -value, and their corresponding 95% confidence interval for each of the selected risk predictors. Based on the multivariate Cox analysis, a nomogram was constructed with the “rms” package in R. The C-index and calibration curve with the bootstrap method were used to evaluate the prediction performance of the nomogram. A $P < 0.05$ was considered statistically significant.

RESULTS

The Common DEMs and Functional Annotation

Of 1,986 immune-related genes obtained from the MSigDB and ImmPort databases, 1,479 genes had corresponding relationships in the TCGA transcriptome. Their expression profiles were used for differential expression analysis (Figure 2A). There were 451 differentially expressed genes in lung tumor and normal tissues, of which 237 were upregulated and 214 were downregulated (Figure 2C). Also, in the GSE68465 dataset, 2,185

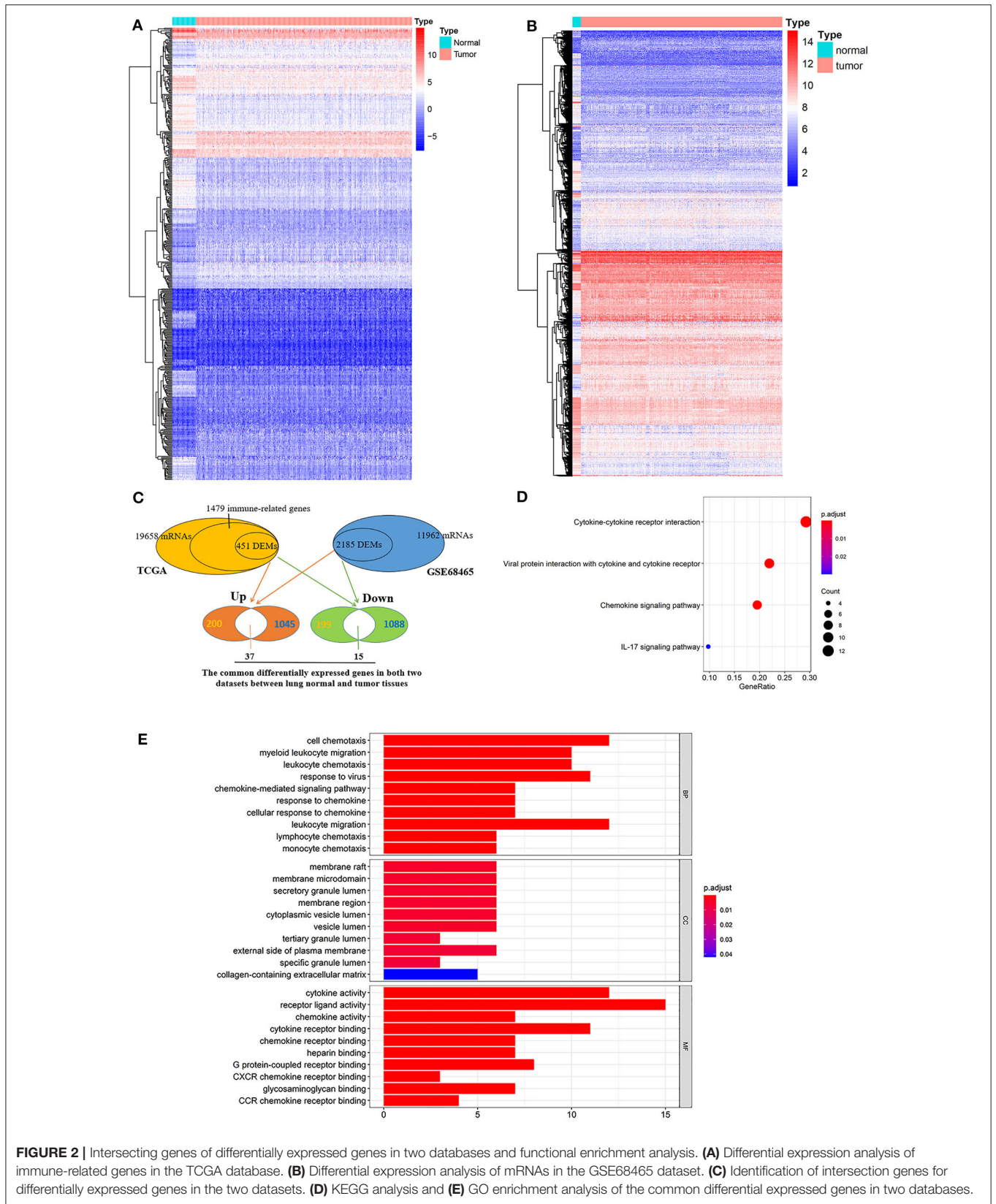


FIGURE 2 | Intersecting genes of differentially expressed genes in two databases and functional enrichment analysis. **(A)** Differential expression analysis of immune-related genes in the TCGA database. **(B)** Differential expression analysis of mRNAs in the GSE68465 dataset. **(C)** Identification of intersection genes for differentially expressed genes in the two datasets. **(D)** KEGG analysis and **(E)** GO enrichment analysis of the common differentially expressed genes in two databases.

genes were differentially expressed in lung tumor and normal tissues (1,082 upregulated genes and 1,103 downregulated genes) (Figures 2B,C).

GO and KEGG enrichment analysis revealed that there were 4 enriched pathways and 361 GO terms (Table S1), of which 4 enrich pathways are shown in Figure 2D and the first 30 GO terms are shown in Figure 2E. KEGG pathway enrichment analysis pointed out that these genes were involved in cytokine–cytokine receptor interaction, viral protein interaction with cytokine and cytokine receptor, chemokine signaling pathway, and IL-17 signaling pathway. Moreover, GO enrichment analysis indicated that these genes were enriched in receptor ligand activity, cell chemotaxis, leukocyte migration, cytokine activity, response to virus, etc.

Robustness of the Novel Signature Based on Four Immune-Related Genes

Six immune-related genes (CD79A, MAL, MMP12, MS4A1, OAS1, and WFDC2) were identified to significantly influence patient outcomes (all $p < 0.05$) in both the TCGA (Figure 3A) and GSE68465 (Figure 3B) datasets and were included in the multivariate Cox analysis (Table S2). After the multivariate Cox analysis (stepwise models), there were finally four genes (MAL, MS4A1, OAS1, and WFDC2) included in the signature according to their risk coefficients (Figure 3C). Of them, the hazard ratios (HRs) of three genes (MAL, MS4A1, and WFDC2) were < 1 , indicating that their overexpression was associated with longer OS, while the other gene (OAS1) with $HR > 1$ had the opposite meaning. The expression of these four genes and their relationship to survival are also shown in Figures 3D,E. The constructed risk score formula is shown $\text{Risk score} = (-0.146 \times \text{ExpressionMAL}) + (-0.227 \times \text{ExpressionMS4A1}) + (0.139 \times \text{ExpressionOAS1}) + (-0.150 \times \text{ExpressionWFDC2})$, through which we estimated the risk score of each patient. Taking the median risk score as the cutoff point, 500 patients were classified into a high-risk group ($n = 250$) and a low-risk group ($n = 250$). The distribution of immune-related genes based on risk score, survival status, and four-gene expression data are shown in Figures 4A–C (development set, $n = 500$), Figures S1A–C (internal validation set, $n = 250$), and Figures S2A–C (external validation set, $n = 442$). The Kaplan–Meier curve analysis in the three datasets obviously demonstrated that patients in the high-risk group had shorter overall survival than those in the low-risk group (log-rank test, all $p < 0.05$; Figure 4D, Figures S1D, S2D). The ROC curves in the development set had a 1-year survival AUC value of 0.718, 3-year survival AUC value of 0.668, and 5-year survival AUC value of 0.652 (Figure 4E). The ROC curves in the internal validation set and external validation set also showed the accuracy of the model in predicting 1-, 3-, and 5-year survival (Figures S1E, S2E). In addition, in three of the four genes (MAL, MS4A1, and WFDC2), their expression value was negatively correlated with the risk score (all $\text{cor} < -0.6$, all $p < 0.001$), while the other gene (OAS1) was opposite ($\text{cor} = 0.358$, $p < 0.001$). Three datasets also showed the same results (Figure 4F, Figures S1F, S2F).

Response of High- and Low-Risk Patients to Chemotherapy and Immunotherapy

According to the pRRophetic algorithm, we predicted the IC50 of six common chemotherapeutic agents (cisplatin, bleomycin, docetaxel, doxorubicin, gemcitabine, and paclitaxel) in high- and low-risk patients and found that all six drugs had higher IC50 in low-risk patients (Wilcoxon test, all $p < 0.05$; Figure 5H). It can be indicated that the high-risk patients were more sensitive to these 6 drugs. In addition, using an online tool TIDE program, TIDE scores were calculated to investigate the effectiveness of immune checkpoint (PD-1 and CTLA-4) inhibitors in immunotherapy in two groups. High-risk patients had markedly lower TIDE score compared with low-risk patients (Wilcoxon test, $p < 0.001$; Figure 5F), indicating that high-risk patients may respond better and had better outcome when receiving immune checkpoint (PD-1 and CTLA-4) inhibitors. In addition, the TMB of high- and low-risk patients was investigated in this study. Tumor mutations in both groups are shown in Figure S3. The results showed that high-risk patients had higher TMB than low-risk patients (Wilcoxon test, $p < 0.001$; Figure 5G).

Differences in Tumor Immune Landscape Between High- and Low-Risk Patients

Comparing the immune infiltration of high- and low-risk groups with two different approaches, we observed that there were significant differences in the components of immune infiltration between the two groups (Figures 5A,B). In the high-risk group, the proportions of iDCs, mast cells, type II IFN response, neutrophils, T helper cells, and inflammatory promoting cells were significantly higher than those of the low-risk group (Wilcoxon test, all $p < 0.05$) (Figure 5A). Similarly, mast cells, eosinophils, neutrophils, and others had higher infiltrations in high-risk groups (Wilcoxon test, all $p < 0.05$) (Figure 5B). Comparing tumor purity and immune score of high- and low-risk patients, we found that LUAD patients in the high-risk group had a lower immune score (Wilcoxon test, $p < 0.001$; Figure 5E) and higher tumor purity (Wilcoxon test, $p < 0.001$; Figure 5D) than patients in the low-risk group. Human leukocyte antigen (HLA) is a major histocompatibility complex (MHC) in humans, closely related to human immune system function, and it also is an important genetic genome of the human immune system. Thus, we further explored the differences in the expression of HLA-related genes between high- and low-risk patients and found that, in addition to HLA-L and HLA-G, the expression levels of other HLA-related genes were significantly different between high- and low-risk groups, that is, these genes had a higher expression in low-risk patients (Wilcoxon test, all $p < 0.05$; Figure 5C). These findings seem to shed light on HLA's important roles in antitumor activity.

We further explored the effects of the four immune-related genes and risk score on the immune infiltration in high- and low-risk patients and found that there was a significant positive correlation between MAL expression level and the infiltration of B cells ($\text{cor} > 0.4$, $p < 0.001$) (Figure S4A) and mast cell resting ($\text{cor} > 0.2$, $p < 0.01$) (Figure S4H). The MS4A1 expression

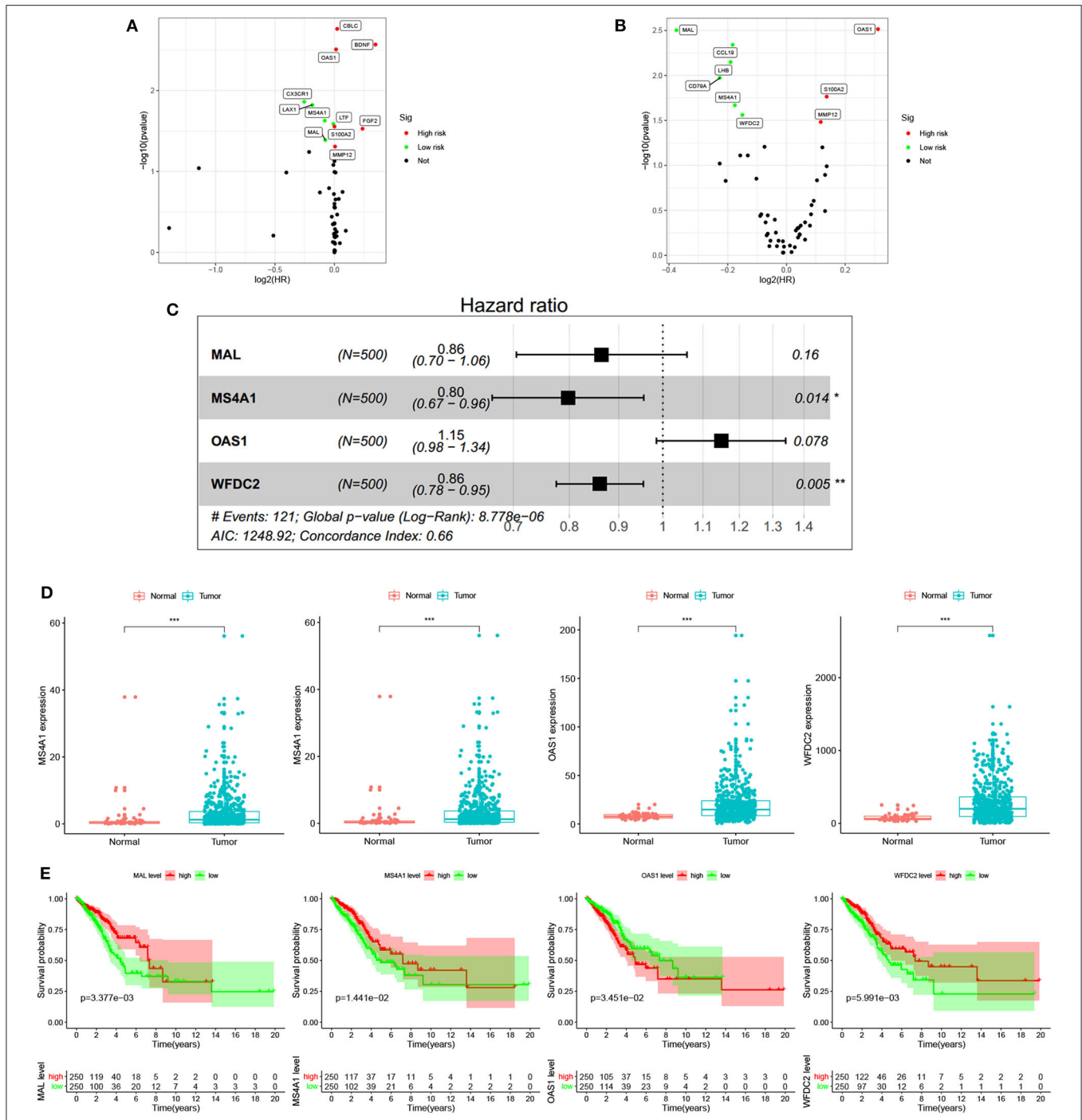
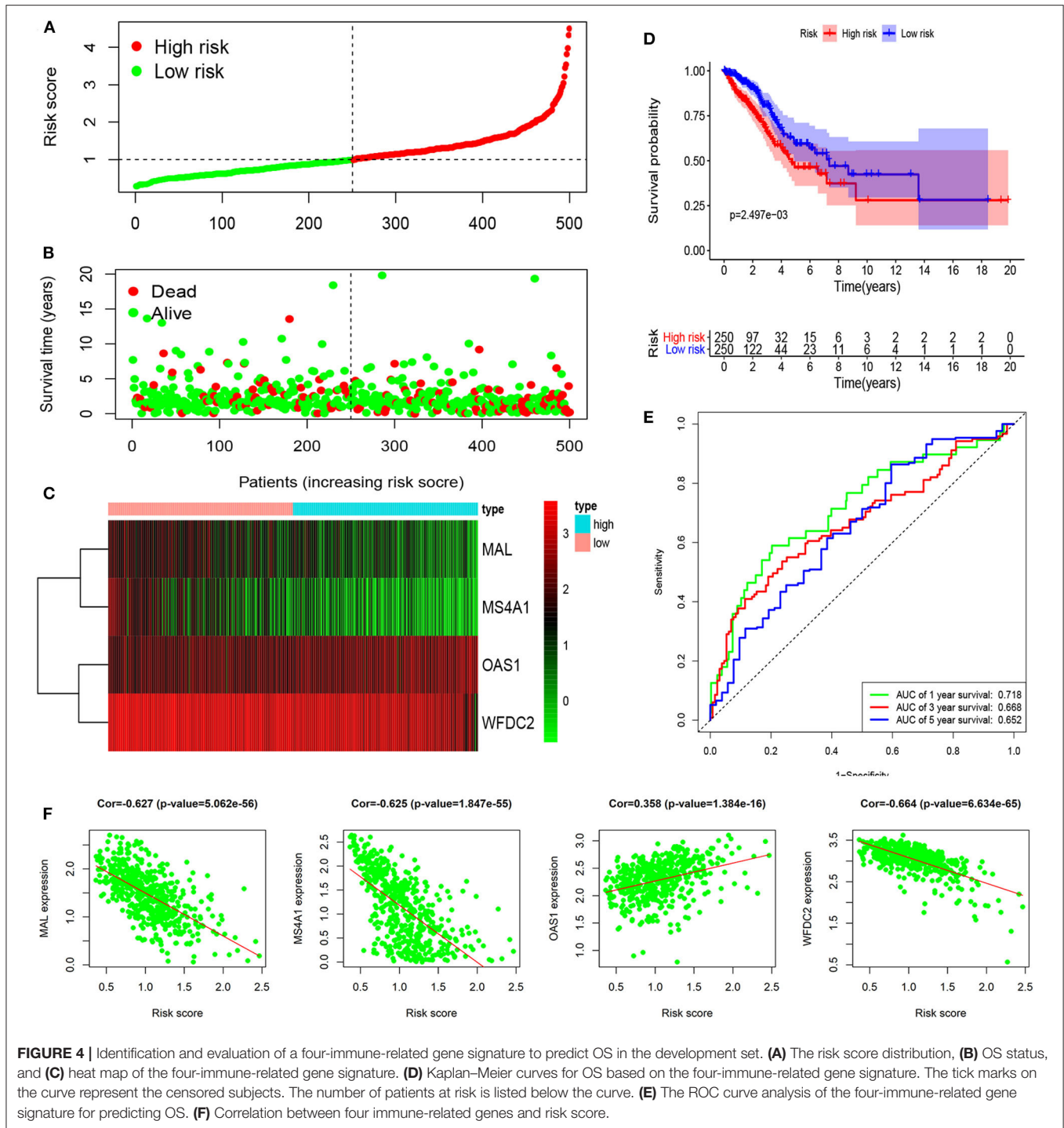


FIGURE 3 | Screening of prognostic immune-related genes and prediction signature construction. Univariate Cox analysis of the common differential expressed genes using the data from the TCGA database (A) and using the data from GEO database (B). Each point represents a gene, where the red point represents a high-risk gene whose overexpression is detrimental to patient prognosis, and green dots have the opposite meaning. (C) Multivariate Cox analysis of genes with prognostic impact in both datasets using the TCGA database expression matrix and clinical information. (D) Differential expression of four immune-related genes (MAL, MS4A1, OAS1, and WFDC2) in the signature between lung normal and tumor tissues. (E) Kaplan-Meier survival analysis of four immune-related genes (MAL, MS4A1, OAS1, and WFDC2) in the signature. (* $p < 0.05$, ** $p < 0.01$, and *** $p < 0.001$).

level was significantly positively correlated with B cells (cor > 0.75, $p < 0.001$) (Figure S4B) and B cell memory (cor > 0.4, $p < 0.001$) (Figure S4I) infiltration. OAS1 expression level and

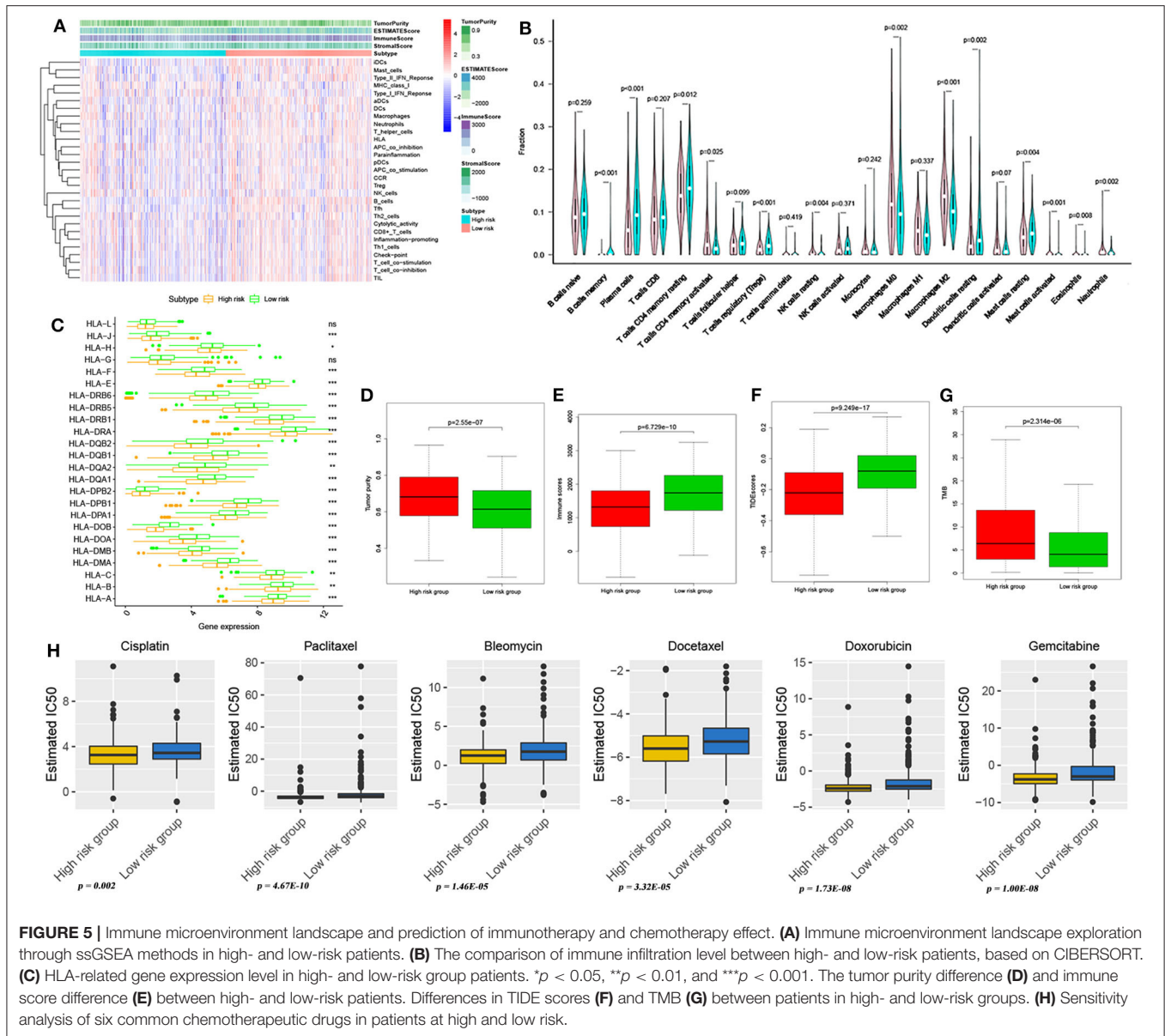
type I IFN response (cor > 0.6, $p < 0.01$) (Figure S4D) as well as macrophage M1 (cor > 0.25, $p < 0.01$) infiltration levels (Figure S4E) were significantly positively correlated. In addition,



WFCD2 expression level was also found to be significantly correlated with iDCs ($cor > 0.3, p < 0.01$) (Figure S4C) and T cells CD4 memory activated ($cor < -0.2, p < 0.0025$) (Figure S4J) infiltration levels. Moreover, risk score and B cells ($cor < -0.5, p < 0.004$) (Figure S4F) as well as NK cells resting ($cor > 0.3, p < 0.005$) (Figure S4G) infiltration level showed significantly related.

Differences in Metabolic Pathways Between High- and Low-Risk Patients

Analysis of hallmark pathway gene signatures indicated that signaling pathways converging at various biological processes were obviously different between high- and low-risk patients. Of note, high-risk patients were more relevant in downregulation of Kras signaling, apical surface, bile acid metabolism, and



myogenesis pathways. In comparison, low-risk patients were preferentially related to E2F targets, G2M checkpoint, MYC targets V1, glycolysis, MYC targets V2, unfolded protein response MTORC1 signaling, and PI3K-AKT-MTOR signaling pathways ($|\log_2FC| > 0.1$, all $p < 0.001$; **Figure 6A**, **Table S3**). In addition, GO gene-set variation analysis revealed that phosphatase activity of inositol triphosphate, inositol polyphosphate 5 phosphatase activity, immunoglobulin complex, and negative regulation of cell-to-fibroblast growth factor chemotaxis of endogenous lipid antigen MHC IB treatment to present lipid antigen binding and alpha beta T cell receptor complex were enriched in the low-risk patients ($|\log_2FC| > 0.1$, all $p < 0.001$; **Figure 6B**, **Table S3**).

Transcription Factors Linked to Four Immune-Related Genes

Most transcription factors (TFs) are associated with the cell cycle and play a vital role in the induction of proto-oncogene and tumor suppressor gene. We obtained 318 TFs from the Cistrome program (<http://cistrome.org/>). By co-expression analysis, we finally identified 45 TFs associated with the four immune-related genes (**Table S4**). Their interrelation is visualized in **Figure 6C**. Of these four genes, the genes co-expressed with the most TFs were MS4A1 ($n = 19$) and WFDC2 ($n = 19$), the least OAS1 ($n = 3$), which could be seen intuitively from the visual network diagram.

to verify the developed nomogram with the C-index of 0.725 (95% CI = 0.668–0.781) in the development set ($n = 500$), 0.793 (95% CI = 0.728–0.858) in the internal validation set ($n = 250$), and 0.679 (95% CI = 0.644–0.714) in the external validation set ($n = 442$), which suggested that the predictive model had good predictive performance. Furthermore, the calibration curves in three datasets also showed good consistency compared with the ideal model, further indicating that the nomogram was stable in predicting the prognosis of LUAD patients (Figures 7B–D).

DISCUSSION

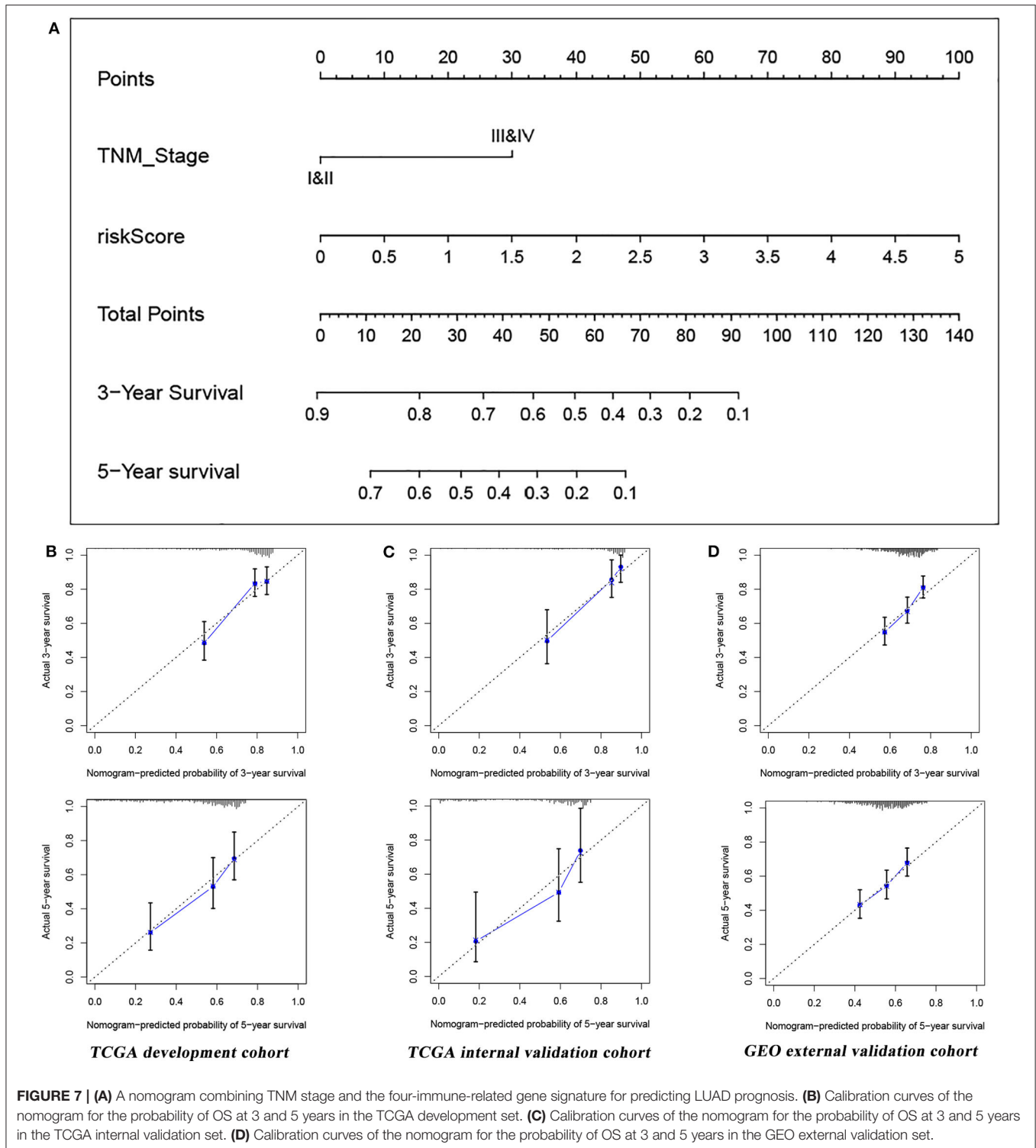
As one of the malignancies with high morbidity and mortality, lung cancer is a public health concern (22, 23). Due to tumor heterogeneity and complex oncogenic mechanisms in LUAD, it is extremely challenging to develop individualized treatment strategies and accurately predict patient prognosis (24, 25). Increasing researches (26–29) have proved that the prognosis of cancer patients was closely related to tumor microenvironment. Immune responses in tumor microenvironments are also considered important determinants of tumor invasiveness and progression. This study constructed a novel immune signature with good robustness, which could accurately distinguish high- and low-risk patients. On this basis, this study explored the tumor immune microenvironment in high- and low-risk patients and revealed that the high-risk patients had higher tumor purity and lower immune score. Tumor purity and immune score were considered to be important factors affecting the prognosis of cancer patients (30–32). Tumor purity refers to the percentage of tumor cells in the tumor immune microenvironment. Some studies have reported that poor prognosis was closely related to low tumor purity in glioma (30) and colorectal cancer (31). Contrary to the poorer prognosis of low tumor purity in glioma and colorectal cancer, Wang et al. (32) observed that patients with low LUAD purity tended to have a better prognosis. This finding was in line with that of our study. Low tumor purity was associated with different outcomes in different cancer patients, which seemed to indicate that the patterns of occurrence and progression of different tumors were also quite different. In our study, high-risk patients with high tumor purity had poor prognosis. We believe that the survival difference between high- and low-risk patients might be due to higher frequency mutations in key pathways and changes in the tumor microenvironment associated with tumor purity.

TABLE 1 | Basic clinicopathologic features.

Characteristics	Subsets	TCGA development set ($n = 500$) (N, %)	TCGA internal validation set ($n = 250$) (N, %)	GEO external validation set ($n = 442$) (N, %)
Age (years)	<65	219 (43.8)	115 (46.0)	214 (48.3)
	≥65	271 (54.2)	129 (51.6)	229 (51.7)
	Unknown	10 (2.0)	6 (0.24)	0 (0.00)
Sex	Female	270 (54.0)	122 (48.8)	220 (49.6)
	Male	230 (46.0)	128 (51.2)	223 (50.4)
T stage	T1&T2	434 (86.8)	218 (87.2)	401 (90.6)
	T3&T4	63 (12.6)	31 (12.4)	40 (9.0)
	Tx	3 (0.6)	1 (0.4)	2 (0.4)
N stage	N0	324 (64.8)	157 (62.8)	229 (67.5)
	N1&N2&N3	165 (33.0)	87 (34.8)	141 (31.9)
	Nx	11 (2.2)	6 (2.4)	3 (0.6)
TNM stage	I&II	387 (77.4)	190 (76.0)	371 (83.8)
	III&IV	105 (21.0)	54 (21.6)	69 (15.6)
	Unknown	8 (1.6)	6 (2.4)	3 (0.6)
Risk score	High risk	250 (50.0)	124 (49.6)	221 (50.0)
	Low risk	250 (50.0)	126 (50.4)	221 (50.0)

TABLE 2 | Univariate and multivariate Cox analysis of the four-immune-related gene signature and clinical risk factors.

Variables	Univariate analysis		Multivariate analysis	
	HR (95% CI)	P-value	HR (95% CI)	P-value
TCGA				
Age (years)	1.012 (0.993–1.032)	0.213	1.020 (1.001–1.040)	0.044
Sex (male vs. female)	0.916 (0.636–1.321)	0.639	0.766 (0.525–1.118)	0.167
T stage (T3&T4 vs. T1&T2)	2.119 (1.315–3.414)	0.002	1.151 (0.669–1.981)	0.612
N stage (N1&N2&N3 vs. N0)	3.161 (2.186–4.569)	<0.001	2.096 (1.354–3.266)	0.001
TNM stage (III&IV vs. I&II)	3.054 (2.099–4.445)	<0.001	1.747 (1.073–2.846)	0.025
Risk score	2.029 (1.654–2.489)	<0.001	1.921 (1.526–2.418)	<0.001
GSE68465				
Age (years)	1.017 (1.004–1.031)	0.013	1.018 (1.004–1.032)	0.010
Sex (male vs. female)	1.224 (0.946–1.584)	0.124	1.051 (0.808–1.368)	0.712
T stage (T3&T4 vs. T1&T2)	1.521 (1.036–2.231)	0.032	1.371 (0.860–2.186)	0.185
N stage (N1&N2&N3 vs. N0)	1.441 (1.107–1.866)	0.007	1.445 (1.057–1.977)	0.021
TNM stage (III&IV vs. I&II)	1.362 (0.983–1.885)	0.063	0.926 (0.588–1.460)	0.742
Risk score	208.6 (21.04–2068.4)	<0.001	192.3 (18.00–2053.7)	<0.001



Additionally, all kinds of cells, cytokines, and chemokines that interact with tumor cells in the tumor microenvironment, especially immune cells, are increasingly recognized as important roles in the body against tumors. Immune score, which can promote the quantification of immune components (such as

immune cells) in tumors, can significantly affect the prognosis of patients. In several studies (32–35), it has been confirmed that high immune scores were associated with better prognosis. Similarly, high-risk patients with worse prognosis had lower immune scores in our study, which further suggested the validity

and accuracy of the signature constructed in this study in identifying high-risk patients. Besides, high-risk patients were significantly different from low-risk patients in terms of immune infiltrating cell types, for example iDCs, mast cells, type II IFN response, neutrophils, T helper cells, macrophages M1, and inflammatory promoting cells. Four immune-related genes (MAL, MS4A1, OAS1, and WFDC2) in the signature were also associated with the immune infiltration. As explained by Aran et al. (36), we also thought that the inflammatory response caused by immune cells might promote the mutation of tumor cells, which in turn affected the prognosis of patients. Therefore, it is still an important part of the future research on LUAD to explore the specific mechanism of tumor immune microenvironment on prognosis.

Since the patients with refractory malignant tumors, including lung cancer (4, 5), benefit significantly from immune checkpoint inhibitors, immunotherapy is becoming a new therapeutic option for cancer patients. TMB and immune checkpoint levels (e.g., PD-1, PD-L1, CTLA4) are considered biomarkers for predicting the efficacy of immunotherapy. As a marker for evaluating the effectiveness of immunotherapy (37), the effect of TMB has been confirmed in the treatment of malignant tumors with mismatch repair defects by the PD-1/PD-L1 antibody (38, 39). TIDE is a completely new computational framework designed by Jiang et al. (16), which can integrate the two immune escape mechanisms of tumor (immune dysfunction and rejection) and is believed to be a substitute for a single biomarker to effectively predict the efficacy of immune checkpoint inhibitors. In view of this, this study assessed the effect of immunotherapy of high- and low-risk patients from two aspects (TMB and TIDE scores) and speculated that high-risk patients may benefit more from immunotherapy. It is worth noting that although immunotherapy can bring good benefits to some lung cancer patients, some patients still do not show the desired results after using immune checkpoint inhibitors (6, 7). The current bottleneck in the treatment of lung cancer also makes such patients have to return to traditional chemotherapy to improve the prognosis. Thus, the mRNA expression data from the TCGA database was used to explore the sensitivity of patients at high and low risk to traditional chemotherapeutic agents (cisplatin, bleomycin, docetaxel, doxorubicin, gemcitabine, and paclitaxel). This study indicated that using the same drugs, the high-risk patients may perform better than the low-risk patients. Currently, platinum-based chemotherapy is the standard regimen for the treatment of advanced LUAD. However, the mechanism of drug resistance and the existence of heterogeneity also make the effect of drug therapy unsatisfactory. This study revealed the sensitivity of high- and low-risk patients to six chemotherapeutic drugs including cisplatin, which would provide a visual field for researchers to develop drugs with high therapeutic index or high efficacy.

In addition, this study found that there were significant differences in metabolic pathways between high- and low-risk patients, such as immunoglobulin complexity and negative regulation of cell-to-fibroblast growth factor chemotaxis of endogenous lipid antigen MHC IB treatment to present lipid antigen binding and alpha beta T cell receptor complex. This

indicated that the pathogenesis of LUAD was a complex biological process driven by specific gene and epigenetic changes. Moreover, abnormal regulation of multiple genes can promote the occurrence and development of LUAD through different mechanisms. Differences in metabolic pathways between high- and low-risk patients based on the established signature have not been previously reported in LUAD, indicating that the four immune-related genes in the signature and varied gene sets in GSEA between high- and low-risk patients have the potential to be further investigated for deeper analysis. In general, these findings may provide a new perspective for researchers and clinicians in finding breakthroughs in further molecular mechanism studies.

For clinical application, good biomarkers should be those that can accurately predict prognosis for patients, distinguish patients with different risks, and thus assist clinicians to make the most reasonable treatment plan in time. Nomogram may be a good choice for this purpose. Nomogram, a visual statistical tool, was widely used in prognostic assessment of cancer patients (40, 41). In this study, combining the immune signature and TNM stage, a prognosis nomogram with excellent performance was constructed. This nomogram incorporated two important predictors (risk score and TNM stage). The TNM stage of patients may be easy to obtain, while the acquisition of another predictor (risk score) required knowledge of the expression of four immune-related genes (MAL, MS4A1, OAS1, and WFDC2) in tumor tissues, which undoubtedly increased the burden of nomogram application. This appears to be a common problem for most molecular diagnostic or prognostic models. How to simplify the clinical application of predictive models is a question for researchers and clinicians to consider. We believe that the development of molecular detection technology in the future is bound to improve this dilemma. The nomogram may be used routinely in the future.

The four immune-related genes in the signature have previously been shown to be potential biomarkers. Relevant researches have reported that deletion of MAL gene expression was associated with the development and progression of many malignancies in humans, such as cervical cancer, ovarian cancer, oral cancer, laryngeal cancer, breast cancer, esophageal cancer, gastric cancer, bowel cancer, and renal cancer (42–49). MS4A1, also known as CD20, is a member of the MS4A gene family. MS4A1 (CD20) is an important marker of B cell differentiation and an important target for immunotherapy in lymphoma (50). Anti-CD20 monoclonal antibody (rituximab) became the first monoclonal antibody approved for cancer treatment in 1997, and it could kill tumor cells by complement-dependent and antibody-dependent cytotoxicity. Along with the development of antibody humanization and Fc segment modification, the therapeutic spectrum is not only limited to lymphoma but also includes chronic lymphoblastic leukemia, acute lymphoblastic leukemia, solid tumor, and immune-related diseases (51–54). OAS1 is an important component of the immune system and has significant antiviral effects. It is worth noting that the relationship between these three genes and LUAD is hardly reported in the literature; however, this study found that all three genes were associated with prognosis in patients with LUAD, and there were significant

differences in gene expression in patients with different clinical features. In combination with the relationship between these three genes and other tumors and the findings of this study, we believe that these three immune-related genes could affect the immune microenvironment of LUAD and might be involved in the occurrence and progression of LUAD. Additionally, along with further exploration, researchers found that WFDC2 presented a high expression state in lung cancer (55–58) and recognized that WFDC2 as a serum tumor marker had important clinical application in the early diagnosis of lung cancer and the monitoring of a curative effect (59). Nevertheless, the expression of WFDC2 in LUAD and its relationship with patients prognosis were rarely reported. This study found that WFDC2 was significantly associated with TNM stage and prognosis in LUAD patients. In general, these four immune-related genes may play key roles in the development of LUAD. This study provided preliminary evidence that these genes were closely related to the clinical features and prognosis of LUAD, which would provide new research directions and ideas for finding new gene therapy targets and developing new antitumor drugs.

There are some limitations in this study. First, although the signature and nomogram constructed in this study using massive data from TCGA and GEO databases have reliable robustness, the nature of retrospective analysis still exists. Second, we explored the immune microenvironment landscape and molecular mechanisms in patients at different risks and predicted their effects of immunotherapy and chemotherapy, but the study still lacked experimental verification.

To make a long story short, this study identified and validated a novel immune-related gene signature comprising four genes (MAL, MS4A1, OAS1, and WFDC2) in LUAD patients, which can serve as a prognostic predictor of LUAD patients. Additionally, the signature can indicate the sensitivity of LUAD patients to chemotherapeutic agents (cisplatin, bleomycin, docetaxel, doxorubicin, gemcitabine, and paclitaxel) as well as immune checkpoint inhibitors and provide new clinical applications for LUAD patients. Furthermore, the established nomogram with good robustness can accurately predict the prognosis of LUAD patients, which may help doctors make more rational treatment decisions.

DATA AVAILABILITY STATEMENT

The datasets presented in this study can be found in online repositories. The names of the repository/repositories and accession number(s) can be found in the article/**Supplementary Material**.

ETHICS STATEMENT

The study was approved by the Institutional Research Committee of Zhongnan Hospital of Wuhan University. Data of our present study was downloaded from the open databases TCGA and GEO, so there was no informed consent from participants. Written informed consent for participation was not required for

this study in accordance with the national legislation and the institutional requirements.

AUTHOR CONTRIBUTIONS

CS, WH, and ZD designed the study. CS analyzed the data and prepared the manuscript. All authors were substantially involved in the research, acquisition of data, analysis, manuscript preparation, and read and approved the final manuscript.

FUNDING

The present study was supported by Zhongnan Hospital of Wuhan University Science Technology and Innovation Cultivating Fund (cxy2017041).

ACKNOWLEDGMENTS

The work benefited from TCGA and GEO databases and other online analytical tools. We are grateful for the access to the resources and the efforts of the staff to expand and improve the databases.

SUPPLEMENTARY MATERIAL

The Supplementary Material for this article can be found online at: <https://www.frontiersin.org/articles/10.3389/fonc.2020.01300/full#supplementary-material>

Figure S1 | Identification and evaluation of a four-immune-related-gene signature to predict OS in the TCGA internal validation set. **(A)** The risk score distribution, **(B)** OS status and **(C)** heatmap of the four-immune-related-gene signature. **(D)** Kaplan-Meier curves for OS based on the four-immune-related-gene signature. The tick-marks on the curve represent the censored subjects. The number of patients at risk is listed below the curve. **(E)** The ROC curve analysis of the four-immune-related-gene signature for predicting OS. **(F)** Correlation between four immune-related genes and risk scores.

Figure S2 | Identification and evaluation of a four-immune-related-gene signature to predict OS in the GEO external validation set. **(A)** The risk score distribution, **(B)** OS status and **(C)** heatmap of the four-immune-related-gene signature. **(D)** Kaplan-Meier curves for OS based on the four-immune-related-gene signature. The tick-marks on the curve represent the censored subjects. The number of patients at risk is listed below the curve. **(E)** The ROC curve analysis of the four-immune-related-gene signature for predicting OS. **(F)** Correlation between four immune-related genes and risk scores.

Figure S3 | Tumor mutations in LUAD patients in TCGA database.

Figure S4 | Correlation of four immune-related genes and risk scores with immune-infiltrating cells. Correlation between MAL **(A)**, MS4A1 **(B)**, WFDC2 **(C)**, OAS1 **(D)**, risk score **(F)** and immune infiltration, based on the ssGSEA approach. Correlation between OAS1 **(E)**, risk score **(G)**, MAL **(H)**, MS4A1 **(I)**, WFDC2 **(J)** and immune-infiltrating cells, based on CIBERSORT.

Figure S5 | Correlation analysis between four immune-related genes and clinical features. There were significant correlations between MAL expression and sex **(A)** and T stage **(B)**. MS4A1 expression was associated with age **(C)**, sex **(D)**, lymph-node metastasis **(E)**, T stage **(F)**, and TNM stage **(G)**. In addition, significant correlations were observed between OAS1 expression and lymph-node metastasis **(H)** and TNM stage **(I)**. WFDC2 expression was associated with TNM stage **(J)**.

Table S1 | GO and KEGG enrichment analysis on the common differentially expressed gene.

Table S2 | Univariate Cox analysis of intersection differentially expressed gene in the TCGA and GEO databases.

Table S3 | Gene set variation analysis in the high- and low-risk groups.

Table S4 | 45 transcription factors associated with the four immune-related genes.

Table S5 | The relationship between four immune-related genes and clinical features.

REFERENCES

- Siegel RL, Miller KD, Jemal A. Cancer statistics, 2020. *CA Cancer J Clin.* (2020) 70:7–30. doi: 10.3322/caac.21590
- Chen R, Xu X, Qian Z, Zhang C, Niu Y, Wang Z, et al. The biological functions and clinical applications of exosomes in lung cancer. *Cell Mol Life Sci.* (2019) 76:4613–33. doi: 10.1007/s00018-019-03233-y
- Finn OJ. Cancer immunology. *N Engl J Med.* (2008) 358:2704–15. doi: 10.1056/NEJMra072739
- Brahmer J, Reckamp KL, Baas P, Crino L, Eberhardt WE, Poddubskaya E, et al. Nivolumab versus docetaxel in advanced squamous-cell non-small-cell lung cancer. *N Engl J Med.* (2015) 373:123–35. doi: 10.1056/NEJMoa1504627
- Hellmann MD, Rizvi NA, Goldman JW, Gettinger SN, Borghaei H, Brahmer JR, et al. Nivolumab plus ipilimumab as first-line treatment for advanced non-small-cell lung cancer (CheckMate 012): results of an open-label, phase 1, multicohort study. *Lancet Oncol.* (2017) 18:31–41. doi: 10.1016/S1470-2045(16)30624-6
- Rooney MS, Shukla SA, Wu CJ, Getz G, Hacohen N. Molecular and genetic properties of tumors associated with local immune cytolytic activity. *Cell.* (2015) 160:48–61. doi: 10.1016/j.cell.2014.12.033
- Li B, Severson E, Pignon JC, Zhao H, Li T, Novak J, et al. Comprehensive analyses of tumor immunity: implications for cancer immunotherapy. *Genome Biol.* (2016) 17:174. doi: 10.1186/s13059-016-1028-7
- Brambilla E, Le Teuff G, Marguet S, Lantuejoul S, Dunant A, Graziano S, et al. Prognostic effect of tumor lymphocytic infiltration in resectable non-small-cell lung cancer. *J Clin Oncol.* (2016) 34:1223–30. doi: 10.1200/JCO.2015.63.0970
- Suzuki K, Kadota K, Sima CS, Nitadori J, Rusch VW, Travis WD, et al. Clinical impact of immune microenvironment in stage I lung adenocarcinoma: tumor interleukin-12 receptor beta2 (IL-12Rbeta2), IL-7R, and stromal FoxP3/CD3 ratio are independent predictors of recurrence. *J Clin Oncol.* (2013) 31:490–8. doi: 10.1200/JCO.2012.45.2052
- Suzuki K, Kachala SS, Kadota K, Shen R, Mo Q, Beer DG, et al. Prognostic immune markers in non-small cell lung cancer. *Clin Cancer Res.* (2011) 17:5247–56. doi: 10.1158/1078-0432.CCR-10-2805
- Shedden K, Taylor JM, Enkemann SA, Tsao MS, Yeatman TJ, Gerald WL, et al. Gene expression-based survival prediction in lung adenocarcinoma: a multi-site, blinded validation study. *Nat Med.* (2008) 14:822–7. doi: 10.1038/nm.1790
- Ritchie ME, Phipson B, Wu D, Hu Y, Law CW, Shi W, et al. Limma powers differential expression analyses for RNA-sequencing and microarray studies. *Nucleic Acids Res.* (2015) 43:e47. doi: 10.1093/nar/gkv007
- Yu G, Wang LG, Han Y, He QY. clusterProfiler: an R package for comparing biological themes among gene clusters. *OmicS.* (2012) 16:284–7. doi: 10.1089/omi.2011.0118
- Sullivan LM, Massaro JM, D'Agostino RS. Presentation of multivariate data for clinical use: the framingham study risk score functions. *Stat Med.* (2004) 23:1631–60. doi: 10.1002/sim.1742
- Geeleher P, Cox NJ, Huang RS. Clinical drug response can be predicted using baseline gene expression levels and *in vitro* drug sensitivity in cell lines. *Genome Biol.* (2014) 15:R47. doi: 10.1186/gb-2014-15-3-r47
- Jiang P, Gu S, Pan D, Fu J, Sahu A, Hu X, et al. Signatures of T cell dysfunction and exclusion predict cancer immunotherapy response. *Nat Med.* (2018) 24:1550–8. doi: 10.1038/s41591-018-0136-1
- Barbie DA, Tamayo P, Boehm JS, Kim SY, Moody SE, Dunn IF, et al. Systematic RNA interference reveals that oncogenic KRAS-driven cancers require TBK1. *Nature.* (2009) 462:108–12. doi: 10.1038/nature08460
- Shen Y, Peng X, Shen C. Identification and validation of immune-related lncRNA prognostic signature for breast cancer. *Genomics.* (2020) 112:2640–6. doi: 10.1016/j.ygeno.2020.02.015
- Hanzelmann S, Castelo R, Guinney J. GSEA: gene set variation analysis for microarray and RNA-seq data. *BMC Bioinformatics.* (2013) 14:7. doi: 10.1186/1471-2105-14-7
- Newman AM, Liu CL, Green MR, Gentles AJ, Feng W, Xu Y, et al. Robust enumeration of cell subsets from tissue expression profiles. *Nat Methods.* (2015) 12:453–7. doi: 10.1038/nmeth.3337
- Lambrechts D, Wauters E, Boeckx B, Aibar S, Nittner D, Burton O, et al. Phenotype molding of stromal cells in the lung tumor microenvironment. *Nat Med.* (2018) 24:1277–89. doi: 10.1038/s41591-018-0096-5
- Torre LA, Siegel RL, Jemal A. Lung cancer statistics. *Adv Exp Med Biol.* (2016) 893:1–19. doi: 10.1007/978-3-319-24223-1_1
- Salavaty A, Rezvani Z, Najafi A. Survival analysis and functional annotation of long non-coding RNAs in lung adenocarcinoma. *J Cell Mol Med.* (2019) 23:5600–17. doi: 10.1111/jcmm.14458
- Yoshizawa A, Motoi N, Riely GJ, Sima CS, Gerald WL, Kris MG, et al. Impact of proposed IASLC/ATS/ERS classification of lung adenocarcinoma: prognostic subgroups and implications for further revision of staging based on analysis of 514 stage I cases. *Mod Pathol.* (2011) 24:653–64. doi: 10.1038/modpathol.2010.232
- Jin X, Di X, Wang R, Ma H, Tian C, Zhao M, et al. RBM10 inhibits cell proliferation of lung adenocarcinoma via RAP1/AKT/CREB signalling pathway. *J Cell Mol Med.* (2019) 23:3897–904. doi: 10.1111/jcmm.14263
- Galon J, Costes A, Sanchez-Cabo F, Kirilovsky A, Mlecnik B, Lagorce-Pages C, et al. Type, density, and location of immune cells within human colorectal tumors predict clinical outcome. *Science.* (2006) 313:1960–4. doi: 10.1126/science.1129139
- Galon J, Fridman WH, Pages F. The adaptive immunologic microenvironment in colorectal cancer: a novel perspective. *Cancer Res.* (2007) 67:1883–6. doi: 10.1158/0008-5472.CAN-06-4806
- Budhu A, Forgues M, Ye QH, Jia HL, He P, Zanetti KA, et al. Prediction of venous metastases, recurrence, and prognosis in hepatocellular carcinoma based on a unique immune response signature of the liver microenvironment. *Cancer Cell.* (2006) 10:99–111. doi: 10.1016/j.ccr.2006.06.016
- Chew V, Chen J, Lee D, Loh E, Lee J, Lim KH, et al. Chemokine-driven lymphocyte infiltration: an early intratumoural event determining long-term survival in resectable hepatocellular carcinoma. *Gut.* (2012) 61:427–38. doi: 10.1136/gutjnl-2011-300509
- Zhang C, Cheng W, Ren X, Wang Z, Liu X, Li G, et al. Tumor purity as an underlying key factor in glioma. *Clin Cancer Res.* (2017) 23:6279–91. doi: 10.1158/1078-0432.CCR-16-2598
- Mao Y, Feng Q, Zheng P, Yang L, Liu T, Xu Y, et al. Low tumor purity is associated with poor prognosis, heavy mutation burden, and intense immune phenotype in colon cancer. *Cancer Manag Res.* (2018) 10:3569–77. doi: 10.2147/CMAR.S171855
- Wang Z, Xu H, Zhu L, He T, Lv W, Wu Z. Establishment and evaluation of a 6-gene survival risk assessment model related to lung adenocarcinoma microenvironment. *Biomed Res Int.* (2020) 2020:6472153. doi: 10.1155/2020/6472153
- Li J, Li X, Zhang C, Zhang C, Wang H. A signature of tumor immune microenvironment genes associated with the prognosis of nonsmall cell lung cancer. *Oncol Rep.* (2020) 43:795–806. doi: 10.3892/or.2020.7464
- Galon J, Pages F, Marincola FM, Thurin M, Trinchieri G, Fox BA, et al. The immune score as a new possible approach for the classification of cancer. *J Transl Med.* (2012) 10:1. doi: 10.1186/1479-5876-10-1
- Angell H, Galon J. From the immune contexture to the Immunoscore: the role of prognostic and predictive immune markers in cancer. *Curr Opin Immunol.* (2013) 25:261–7. doi: 10.1016/j.coi.2013.03.004
- Aran D, Sirota M, Butte AJ. Systematic pan-cancer analysis of tumour purity. *Nat Commun.* (2015) 6:8971. doi: 10.1038/ncomms9971

37. Carbone DP, Reck M, Paz-Ares L, Creelan B, Horn L, Steins M, et al. First-line nivolumab in stage IV or recurrent non-small-cell lung cancer. *N Engl J Med.* (2017) 376:2415–26. doi: 10.1056/NEJMoa1613493
38. Le DT, Durham JN, Smith KN, Wang H, Bartlett BR, Aulakh LK, et al. Mismatch repair deficiency predicts response of solid tumors to PD-1 blockade. *Science.* (2017) 357:409–13. doi: 10.1126/science.aan6733
39. Le DT, Uram JN, Wang H, Bartlett BR, Kemberling H, Eyring AD, et al. PD-1 blockade in tumors with mismatch-repair deficiency. *N Engl J Med.* (2015) 372:2509–20. doi: 10.1056/NEJMoa1500596
40. Liang W, Zhang L, Jiang G, Wang Q, Liu L, Liu D, et al. Development and validation of a nomogram for predicting survival in patients with resected non-small-cell lung cancer. *J Clin Oncol.* (2015) 33:861–9. doi: 10.1200/JCO.2014.56.6661
41. Balachandran VP, Gonen M, Smith JJ, DeMatteo RP. Nomograms in oncology: more than meets the eye. *Lancet Oncol.* (2015) 16:e173–80. doi: 10.1016/S1470-2045(14)71116-7
42. Mimori K, Shiraishi T, Mashino K, Sonoda H, Yamashita K, Yoshinaga K, et al. MAL gene expression in esophageal cancer suppresses motility, invasion and tumorigenicity and enhances apoptosis through the Fas pathway. *Oncogene.* (2003) 22:3463–71. doi: 10.1038/sj.onc.1206378
43. Horne HN, Lee PS, Murphy SK, Alonso MA, Olson JJ, Marks JR. Inactivation of the MAL gene in breast cancer is a common event that predicts benefit from adjuvant chemotherapy. *Mol Cancer Res.* (2009) 7:199–209. doi: 10.1158/1541-7786.MCR-08-0314
44. Overmeer RM, Henken FE, Bierkens M, Wilting SM, Timmerman I, Meijer CJ, et al. Repression of MAL tumour suppressor activity by promoter methylation during cervical carcinogenesis. *J Pathol.* (2009) 219:327–36. doi: 10.1002/path.2598
45. Lee PS, Teaberry VS, Bland AE, Huang Z, Whitaker RS, Baba T, et al. Elevated MAL expression is accompanied by promoter hypomethylation and platinum resistance in epithelial ovarian cancer. *Int J Cancer.* (2010) 126:1378–89. doi: 10.1002/ijc.24797
46. Beder LB, Gunduz M, Hotomi M, Fujihara K, Shimada J, Tamura S, et al. T-lymphocyte maturation-associated protein gene as a candidate metastasis suppressor for head and neck squamous cell carcinomas. *Cancer Sci.* (2009) 100:873–80. doi: 10.1111/j.1349-7006.2009.01132.x
47. Buffart TE, Overmeer RM, Steenbergen RD, Tijssen M, van Grieken NC, Snijders PJ, et al. MAL promoter hypermethylation as a novel prognostic marker in gastric cancer. *Br J Cancer.* (2008) 99:1802–7. doi: 10.1038/sj.bjc.6604777
48. Llorente A, de Marco MC, Alonso MA. Caveolin-1 and MAL are located on prostasomes secreted by the prostate cancer PC-3 cell line. *J Cell Sci.* (2004) 117:5343–51. doi: 10.1242/jcs.01420
49. de Marco MC, Martin-Belmonte F, Kremer L, Albar JP, Correias I, Vaerman JP, et al. MAL2, a novel raft protein of the MAL family, is an essential component of the machinery for transcytosis in hepatoma HepG2 cells. *J Cell Biol.* (2002) 159:37–44. doi: 10.1083/jcb.200206033
50. Thomas DA, O'Brien S, Kantarjian HM. Monoclonal antibody therapy with rituximab for acute lymphoblastic leukemia. *Hematol Oncol Clin North Am.* (2009) 23:949–71. doi: 10.1016/j.hoc.2009.07.005
51. Lee JJ, Lam MS, Rosenberg A. Role of chemotherapy and rituximab for treatment of posttransplant lymphoproliferative disorder in solid organ transplantation. *Ann Pharmacother.* (2007) 41:1648–59. doi: 10.1345/aph.1K175
52. Jabbour E, O'Brien S, Ravandi F, Kantarjian H. Monoclonal antibodies in acute lymphoblastic leukemia. *Blood.* (2015) 125:4010–6. doi: 10.1182/blood-2014-08-596403
53. Seiter K, Mamorska-Dyga A. Obinutuzumab treatment in the elderly patient with chronic lymphocytic leukemia. *Clin Interv Aging.* (2015) 10:951–61. doi: 10.2147/CIA.S69278
54. Battella S, Cox MC, Santoni A, Palmieri G. Natural killer (NK) cells and anti-tumor therapeutic mAb: unexplored interactions. *J Leukoc Biol.* (2016) 99:87–96. doi: 10.1189/jlb.5VMR0415-141R
55. Wojcik E, Tarapacz J, Rychlik U, Stasik Z, Sas-Korczynska B, Skotnicki P, et al. Human epididymis protein 4 (HE4) in patients with small-cell lung cancer. *Clin Lab.* (2016) 62:1625–32. doi: 10.7754/Clin.Lab.2016.151212
56. Choi SI, Jang MA, Jeon BR, Shin HB, Lee YK, Lee YW. Clinical usefulness of human epididymis protein 4 in lung cancer. *Ann Lab Med.* (2017) 37:526–30. doi: 10.3343/alm.2017.37.6.526
57. Huang W, Wu S, Lin Z, Chen P, Wu G. Evaluation of HE4 in the diagnosis and follow up of non-small cell lung cancers. *Clin Lab.* (2017) 63:461–7. doi: 10.7754/Clin.Lab.2016.160818
58. Zhong H, Qian Y, Fang S, Yang L, Li L, Gu W. HE4 expression in lung cancer, a meta-analysis. *Clin Chim Acta.* (2017) 470:109–14. doi: 10.1016/j.cca.2017.05.007
59. Zeng Q, Liu M, Zhou N, Liu L, Song X. Serum human epididymis protein 4 (HE4) may be a better tumor marker in early lung cancer. *Clin Chim Acta.* (2016) 455:102–6. doi: 10.1016/j.cca.2016.02.002

Conflict of Interest: The authors declare that the research was conducted in the absence of any commercial or financial relationships that could be construed as a potential conflict of interest.

Copyright © 2020 Song, Guo, Yu, Wang, Wang, Dong and Hu. This is an open-access article distributed under the terms of the Creative Commons Attribution License (CC BY). The use, distribution or reproduction in other forums is permitted, provided the original author(s) and the copyright owner(s) are credited and that the original publication in this journal is cited, in accordance with accepted academic practice. No use, distribution or reproduction is permitted which does not comply with these terms.